Current Biology, Vol. 12, 540–550, April 2, 2002, ©2002 Elsevier Science Ltd. All rights reserved. PII S0960-9822(02)00759-5

Circadian Cycling of the Mouse Liver Transcriptome, as Revealed by cDNA Microarray, Is Driven by the Suprachiasmatic Nucleus

Ruth A. Akhtar,[1,6] Akhilesh B. Reddy,[2,6] Elizabeth S. Maywood,[2] Jonathan D. Clayton,[1] Verdun M. King,[3] Andrew G. Smith,[4] Timothy W. Gant,[4] Michael H. Hastings,[2] and Charalambos P. Kyriacou[1,5]

[1]Department of Genetics
University of Leicester
Leicester LE1 7RH
[2]Neurobiology Division
MRC Laboratory of Molecular Biology
Hills Road
Cambridge CB2 2QH
[3]Department of Anatomy
University of Cambridge
Cambridge CB2 3DY
[4]MRC Toxicology Unit
University of Leicester
Leicester LE1 9HN
United Kingdom

Summary

Background: Genes encoding the circadian pacemaker in the hypothalamic suprachiasmatic nuclei (SCN) of mammals have recently been identified, but the molecular basis of circadian timing in peripheral tissue is not well understood. We used a custom-made cDNA microarray to identify mouse liver transcripts that show circadian cycles of abundance under constant conditions.

Results: Using two independent tissue sampling and hybridization regimes, we show that ~9% of the 2122 genes studied show robust circadian cycling in the liver. These transcripts were categorized by their phase of abundance, defining clusters of day- and night-related genes, and also by the function of their products. Circadian regulation of genes was tissue specific, insofar as novel rhythmic liver genes were not necessarily rhythmic in the brain, even when expressed in the SCN. The rhythmic transcriptome in the periphery is, nevertheless, dependent on the SCN because surgical ablation of the SCN severely dampened or destroyed completely the cyclical expression of both canonical circadian genes and novel genes identified by microarray analysis.

Conclusions: Temporally complex, circadian programming of the transcriptome in a peripheral organ is imposed across a wide range of core cellular functions and is dependent on an interaction between intrinsic, tissue-specific factors and extrinsic regulation by the SCN central pacemaker.

[5]Correspondence: cpk@leicester.ac.uk
[6]These authors contributed equally to this work.

Introduction

In mammals, circadian rhythms are generated by a central pacemaker in the suprachiasmatic nuclei (SCN) of the hypothalamus [1, 2]. The SCN impose temporal structure across the brain and peripheral organs via neural and endocrine outputs. Disruption of this temporal programming of physiology and behavior, as occurs during rotational shift work, jet lag, and old age, carries major costs for human health [3, 4, 5]. An important goal, therefore, is to identify the physiological basis of circadian rhythmicity in peripheral tissues and its relationship to the SCN. In invertebrates and lower vertebrates, circadian rhythms in the periphery are driven by tissue-autonomous circadian oscillators, often light sensitive, and synchronized to but not dependent on central pacemakers [6, 7]. Recent studies using transgenic rodents and fibroblast cell lines indicate that peripheral tissues of mammals may also have a limited autonomous capacity for circadian gene expression [8, 9], but the relationship with the central pacemaker of the SCN is not yet defined.

Analysis of central and peripheral clock mechanisms has received an enormous impetus from the recent identification of mammalian "clock genes" [1]. Many have circadian rhythms of expression, and their products are involved in complex autoregulatory feedback loops involving both negative and positive controls [1]. Cycling mRNAs are not, however, limited to the circadian oscillator itself, and a number of rhythmically expressed clock output genes have been reported [1, 10, 11]. Systematic attempts to identify genes that show circadian cycles of mRNA expression have been made in *Neurospora*, *Drosophila*, mouse, and cyanobacteria, using differential/subtractive screens or reporter gene insertions [12-15]. In *Arabidopsis,* high-density oligonucleotide and EST microarrays have been used to scan ~8000 genes and have revealed that 2%–6% undergo circadian cycles of transcription [16, 17]. We employed a cDNA microarray, customized for the analysis of liver function, to scan ~5% of the mouse genome in order to characterize circadian transcriptional cycling in the liver under constant environmental conditions. We validated circadian expression patterns using in situ hybridization in both liver and brain and tested their dependence on the central pacemaker by analyzing tissues from SCN-lesioned mice.

Results

Microarray Analysis Reveals Circadian Transcriptional Cycling in the Liver

Rhythmic genes were revealed by two independent sampling and analysis strategies. An "anchored" comparison considered the relative change in mRNA abundance between CT0 and all other time points and when plotted yielded a conventional image of cyclical gene expression (Figures 1B and 1C, right-hand panels). The

moving window" analyses scanned across the circadian cycle comparing the relative abundance of mRNA expression between two samples 12 hr apart. For rhythmic genes, this yielded a linear plot as the comparison moved from peak:trough, through midpoint:midpoint to trough:peak, or vice versa depending on phase (Figures 1B and 1C, left-hand panels). The amplitude of changes revealed by this moving window analysis was ~2-fold greater than the anchored comparison, because it was likely to incorporate a comparison of the two extreme levels of gene expression within the cycle. For the two strategies, statistically significant cycles of expression were revealed by spectral (anchored) and cross-correlation (moving window) analyses (see Experimental Procedures). Only genes confirmed as rhythmic by both approaches were considered. Of 2122 genes sampled, 187 (8.8%) gave significantly rhythmic profiles. Although we did not discriminate with respect to amplitude, 32 genes showed <1.5-fold amplitude (peak to trough), while 19 revealed an amplitude >4-fold.

Hierarchical cluster analysis of the anchored data [18] revealed eight clusters (Figure 1A and Table S3 in the Supplementary Material available with this article online). Clusters 1 through 3 include genes whose transcripts peak in expression between CT14-18 and include *mPer1* (cluster 2) and *mPer2* (cluster 3) (Figures 1A and 1B). The large cluster 4 has an earlier peak (CT10-14) and includes *Ltbr* and *Vcam*, while cluster 5 includes *Arnt-like* (*Bmal1*), which characteristically peaks in antiphase to *Per* (Figure 1C) [19]. It is clear from these data that the transcriptional profile of the liver changes systematically and progressively through the circadian cycle.

There was an interaction between the phase of peak expression and the amplitude of expression. Whereas genes with amplitudes of less than 2-fold tended to peak around CT18, there was a significant tendency for genes with higher amplitudes to peak at CT02 and CT14, reflecting the subjective light/dark transitions (Figure 1D). A striking observation is that the three most dramatic cycles in terms of amplitude were those corresponding to *Bmal1* (15-fold), *mPer1* (9-fold), and *insulin-like growth factor binding protein-1* (22-fold). The canonical clock genes *mPer2* (7-fold) and *mPer3* (4-fold) followed closely behind. This implies that canonical clock genes may present the highest amplitudes within the cycling gene subset of peripheral tissues.

Independent Corroboration of Transcriptional Cycling by In Situ Hybidization

In situ hybridization was used to cross-validate the cycles observed on the arrays for two canonical genes (*mPer2* and *Bmal1*) and three novel cycling genes, *Nfix*, *Pnp*, and a sequence similar to rat *brain specific polypeptide R19* (*bspR19*). These novel genes were selected because they exhibited cycles of modest amplitude (between 1.45- and 1.76-fold) and were in phase with one or other of the canonicals. Examination of their expression pattern by in situ hybridization would therefore provide a rigorous, independent test of the array data on a third group of animals. As anticipated, *mPer2* and *Bmal1* were "expressed with high amplitude and showed statistically significant circadian rhythms in the liver (Figure 2A). Moreover, for both genes, there was a significant statistical correlation between the relative changes in mRNA expression as determined by the microarray and by the in situ signal. The novel genes also exhibited statistically significant circadian expression profiles peaking in late subjective day (*Nfix* and *bspR19*) or late subjective night (*Pnp*). As for the canonical clock genes, there was a direct correlation between the array and in situ hybridization data for the novel rhythmic genes. The circadian cycles of gene expression revealed independently by the two strategies for microarray analysis were therefore corroborated by in situ hybridization.

A Subset of Novel Liver Circadian Genes Is Also Expressed in the SCN

To explore potential contribution to pacemaker function, the expression of the three novel genes in the SCN was examined. Whereas the canonical clock genes were expressed in the SCN with high-amplitude cycles (Figure 2B), of the three novel genes, *Pnp* was expressed at a modest level, whereas expression of *Nfix* and *bspR19* was low, and none exhibited a statistically significant circadian rhythm in the SCN. We then examined the striatum, a structure intimately involved in the expression of spontaneous locomotion. As anticipated, the canonical genes again showed a statistically significant circadian expression pattern in the striatum, peaking at CT12 (*mPer2*) or CT4 (*mBmal1*). Expression of *Nfix* and *bspR19* was constitutive, but *Pnp* exhibited a significant circadian cycle of expression, peaking around CT12-16 (Figure 2B).

To examine tissue-specific circadian regulation further, we conducted moving window and anchored comparisons on RNA samples from hypothalami collected from mice across the second circadian cycle in DR:DR and hybridized to the microarray. We focused our attention on the 187 genes that were rhythmically expressed in the liver. Of these, only 19 (~10%) including *mPer1-3* and *Bmal1* were also identified by both array strategies as rhythmic in the hypothalamus. None of the three novel genes tested by in situ hybridization of the liver and brain (*Nfix*, *Pnp*, and *bspR19*) were rhythmic, either by array or by in situ analysis (Figure 2). Of the other novel liver genes, those with amplitudes greater than 2-fold in the hypothalamus include *Timp3*, *Tff1*, *Ubce7*, *Wee1* homolog, *Ap1b1*, and *Tubb4*. All except *Wee1* (which had similar phases in both tissues) showed between 6 to 10 hr delays in their oscillation in the liver compared to the brain (data not shown). These results demonstrate that the potential for circadian expression of these clock-regulated genes is tissue dependent.

Transcriptional Cycling of Novel Circadian Genes in the Liver Is Dependent on the SCN

To examine the role of the SCN in circadian regulation of liver transcriptional cycles, liver mRNA was extracted from mice that had sustained bilateral surgical ablation of the SCN (Figure 3A). χ^2 periodogram analysis confirmed the loss of circadian activity/rest cycles in lesioned animals, and the extent of the lesion was determined by post-hoc histological analysis (Figures 3A and

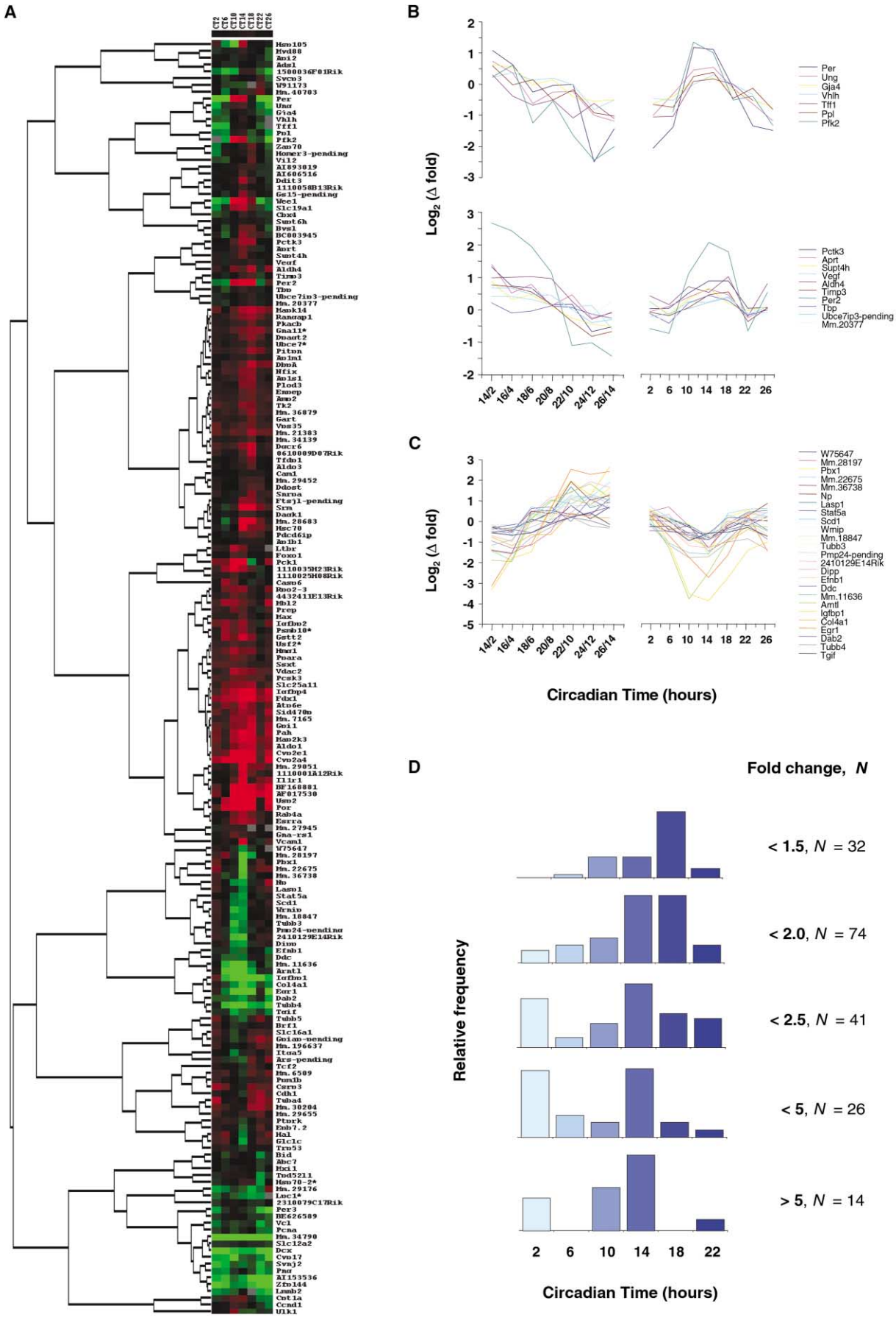
A
CT2
CT6
CT10
CT14
CT18
CT22
CT26
B
Log2 (Δ fold)
Per
Ung
Gja4
Vhlh
Tff1
Ppl
Pfk2
Pctk3
Aprt
Slpt4h
Vegf
Aldh4
Timp3
Per2
Tbp
Ubce7ip3-pending
Mm.20377
14/2
16/4
18/6
20/8
22/10
24/12
26/14
2
6
10
14
18
22
26
C
Log2 (Δ fold)
W75647
Mm.28197
Pbx1
Mm.22675
Mm.36738
Np
Lasp1
Stat5a
Scd1
Wrnip
Mm.18847
Tubb3
Pmp24-pending
2410129E14Rik
Dipp
Efnb1
Ddc
Mm.11636
Arntl
Igfbp1
Col4a1
Egr1
Dab2
Tubb4
Tgif
Circadian Time (hours)
D
Fold change, N
Relative frequency
< 1.5, N = 32
< 2.0, N = 74
< 2.5, N = 41
< 5, N = 26
> 5, N = 14
2
6
10
14
18
22
Circadian Time (hours)

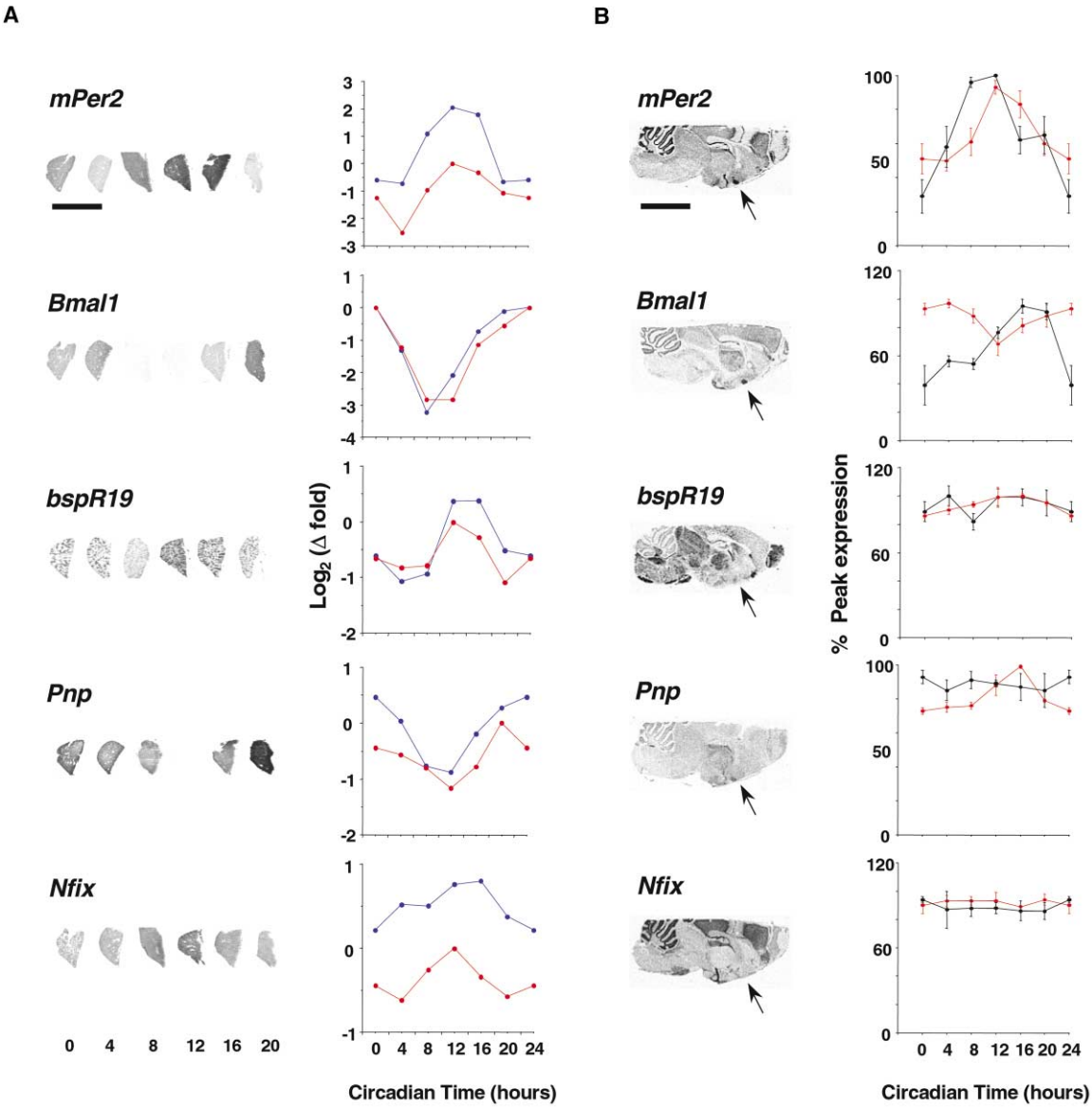

Figure 2. Analysis of Gene Expression Cycles in Liver and Brain by In Situ Hybridization

(A) Representative autoradiographs of liver tissue probed for two canonical clock genes, *mPer2* and *Bmal1*, and three novel, rhythmically expressed genes identified by microarray analyses. Mean hybridization signal (red line, n = 3 mice per time point) is plotted as fold change (expressed as a base 2 logarithm) in order to compare with array data (blue line). All five genes exhibited a statistically significant circadian rhythm of expression (ANOVA, $p < 0.05$) that corresponded directly, in terms of phase and relative amplitude, with the circadian cycle revealed by array analysis. Scale bar, 10 mm.

(B) Representative autoradiographs of brain sections probed for the same five genes (*Bmal1* sampled at CT16, the rest at CT12). Arrows indicate location of SCN, clearly evident in *mPer2* and *Bmal1* images. Mean SCN hybridization signal (black line, ± SEM, n = 3 mice per time point; n = 1 for *bspR19*, where errors represent error around replicate measures for single brain). Both canonical genes were highly rhythmic in the SCN (ANOVA, $p < 0.01$). In contrast, none of the novel genes were rhythmically expressed in the SCN, even though some specific hybridization signal was evident. The two canonical clock genes were also expressed rhythmically in the striatum (red line, mean ± SEM, n = 3 mice per sample, except *bspR19*, as above). The novel gene *Pnp* was also expressed rhythmically in the striatum, peaking in the active phase of circadian night (ANOVA, $p < 0.05$). Scale bar, 8 mm.

Figure 1. Circadian Gene Expression Profiles in Mouse Liver

(A) Global hierarchical cluster analysis of genes expressed in liver on a circadian basis. See Supplementary Material for further details. Representative clusters of (B) day- and (C) night-phased gene expression rhythms, revealed by moving window (left panels) and anchored comparison (right panels) plots. (Δ fold represents a [Cy5/Cy3] fluorophore ratio.) (D) Circadian distribution of peak phases in genes ordered on basis of cycle amplitude, ranging from lowest (<1.5-fold) to highest (>5-fold) amplitudes. The group size is given as N. The χ^2 heterogeneity value ($\chi^2 = 51.3$, d.f. = 20, $p < 0.001$) reveals a significant difference in the distribution of phases between the different amplitude groups.

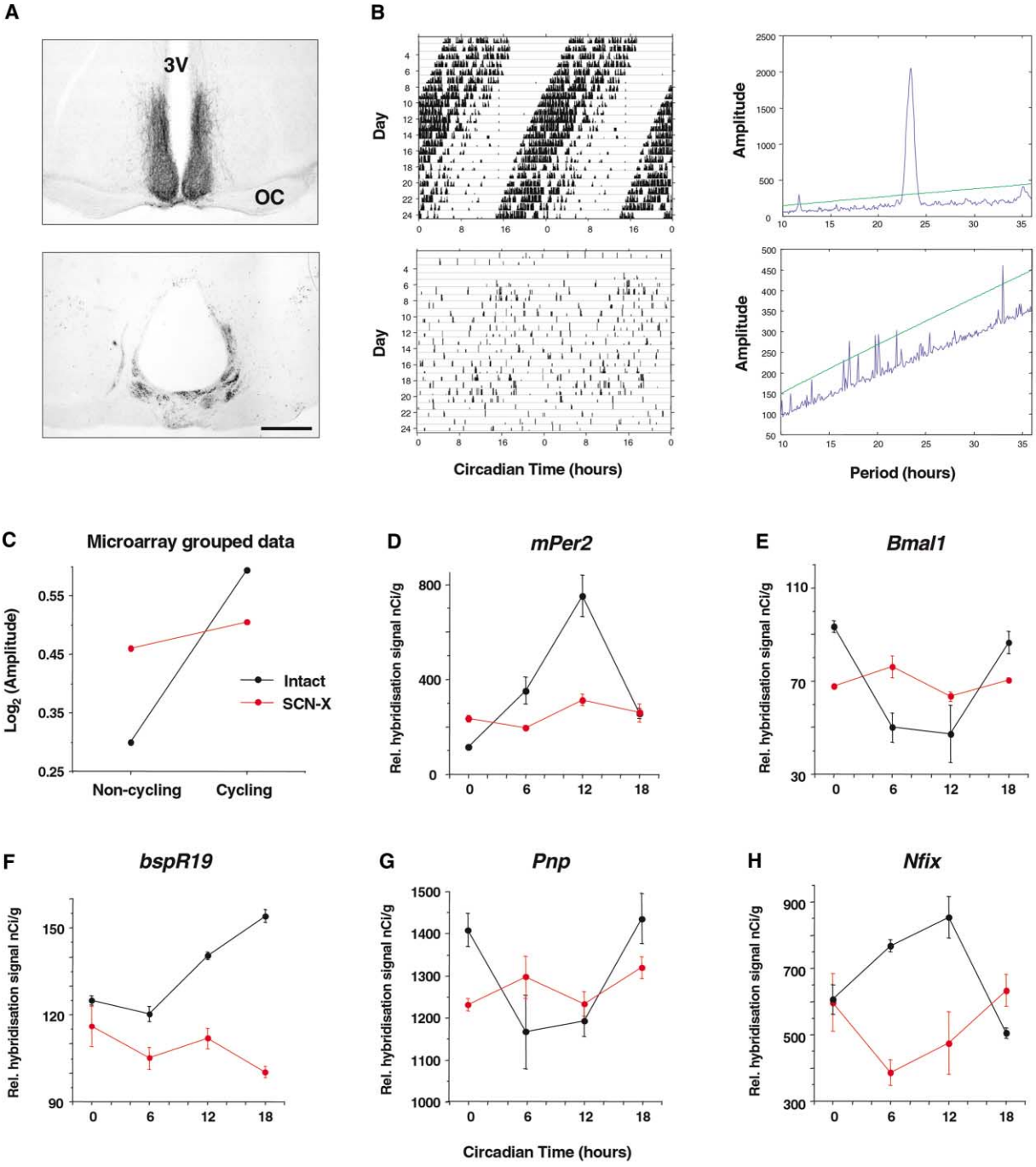

Figure 3. Effect of SCN Ablation on Circadian Behavior and Liver Gene Expression

(A) Representative coronal sections of hypothalamus in intact and SCN-X mice immunostained for the neuropeptide PHI to identify the SCN and efferent fibers. Note the clear definition of SCN and efferents in intact brain and their complete absence after SCN ablation. The peroxidase reaction product within necrotic tissue around the lesion site is nonspecific (3V, third ventricle; OC, optic chasm; scale bar, 500 μm).

(B) Representative double-plotted actograms and corresponding χ^2 periodograms from intact and SCN-X mice, free-running in DR:DR, confirm behavioral arrhythmia induced by SCN ablation.

(C) Effect of SCN-X on rhythmic gene expression identified by microarray analysis. In the intact mice, the rhythmic and nonrhythmic gene clusters showed a very large difference in amplitude of expression. In SCN-lesioned mice, this difference between the two groups of genes was completely abolished, demonstrating the loss of circadian expression across the transcriptome as sampled.

(D–H) Individual gene cycles in livers of intact (black line) and SCN-X (red line) mice examined by in situ hybridization. (D) *mPer2*; (E) *Bmal1*; (F) sequence similar to brain-specific polypeptide R19, *bspR19* (Unigene accession number Mm.28040); (G) purine nucleoside phosphorylase, *Pnp*; (H) nuclear factor I/X, *Nfix*. In all cases, data are plotted as mean ± SEM derived from n = 3 mice. The control intact mice were independent of those presented in Figure 2. Two-way ANOVA revealed lesion and/or lesion versus time interaction for all five genes tested, confirming loss of circadian regulation following SCN ablation.

3B). Tissues were sampled on the second cycle in continuous darkness at projected CT0, CT6, CT12, or CT18, and extracted RNA hybridized to the microarray using the anchored comparison between CT0/CT6 and CT0/CT18. To avoid comparing data directly between two array experiments performed under different hybridization conditions, we obtained a measure of amplitude for cycling genes versus noncycling genes and compared it between lesioned and intact animals. We thus identified genes from our first anchored experiment that cycled with a peak in the liver at CT6 and CT18 and subtracted the Cy5/Cy3 ratio from the corresponding CT0/CT6 and CT0/CT18 points, obtaining a measure of rhythm amplitude. We then compared this amplitude to that obtained from those same CT points, from our pool of "noncycling" liver genes in the intact group. Next, we calculated the corresponding amplitudes generated from the SCN-lesioned animals, by taking those same cycling genes that peak in intact mice at CT6 and CT18 and comparing them with the same noncycling genes from the experimental subjects. Two-way ANOVA (cycling versus noncycling, intact versus lesioned) produced a significant interaction [$F_{(1, 1130)} = 7.55$, $p = 0.006$], revealing that the large difference in amplitude between cycling and noncycling genes in intact mice was lost in SCN-ablated animals (Figure 3C. n.b. the difference in overall amplitude between the two experiments simply reflects inevitable slight differences in hybridization conditions). In addition, we compared similar moving window data for each cycling gene that peaked at CT0 or CT12 and CT6 or CT18 from ablated and intact animals. We observed that in 94% of the cases, the amplitude was lower in the surgically treated animals on a gene-by-gene basis (data not shown), confirming the results from the anchored data. Consequently, ablation of the SCN severely dampens the amplitude of circadian cycling mRNAs in a peripheral tissue. To extend this result, we conducted in situ hybridization for the canonical clock genes *mPer2* and *Bmal1* and the novel cycling genes *Pnp*, *Nfix*, and *bspR19* on the livers of the SCN-lesioned animals, sampled on the second cycle in DR:DR, and compared them to a further, independent series of tissues from intact controls. As anticipated, the high-amplitude circadian profiles of the canonical clock genes observed in intact animals were dramatically attenuated in the livers of SCN-lesioned mice, although both *mPer2* and *Bmal1* maintained a statistically significant circadian cycle (Figures 3D and 3E). In control tissues, the novel cycling genes again exhibited statistically significant circadian cycles (see Figure 2), but this was lost following ablation of the SCN, and levels remained around the basal values observed in the livers of intact animals. This indicates that efferent control from the SCN is necessary not only for circadian patterning but also for positive regulation of these clock-controlled genes.

Identified Novel Circadian Genes Have a Diverse Range of Functions

Having identified a set of cyclical transcripts in the liver, we sought to characterize them into functional groups according to the known or predicted role of their products (see Table S3, Figure 4A). A striking finding was that several genes encoding components of key metabolic pathways exhibited robust transcriptional cycling in the liver, including three genes in the glycolysis pathway: *6-phosphofructokinase-2* (*Pfk-2*), *aldolase* (two isoforms, *Aldo1* and *Aldo3*), and *glucose phosphate isomerase* (*Gpi*) (Figure 4B). These functionally related genes have expression peaks at the subjective day/night transition and in the subjective night, corresponding to the active, ingestive phase of the animals. We also identified many genes encoding essential structural elements within cells, including four tubulin subunit monomers (*Tuba4*, *Tubb3*, *Tubb4*, and *Tubb5*), *Disabled-2* (*Dab2*) and *LIM and SH3 protein 1* (*Lasp1*), the majority of which clustered with a pronounced nadir at CT14 (Figure 4C). Several genes involved in vesicle transport and endocytosis were also identified in the circadian transcriptome (Figure 4D). Various subunits of the AP-1 adaptor protein complex (*Ap1b1*, *Ap1m1*, and *Ap1s1*) have modest rhythms of gene expression that cycle in phase with each other, peaking half-way through the subjective night at CT18. *Synaptojanin 2* (*Synj2*) expression follows a similar pattern, with its peak occurring earlier, between CT10 and CT18. In contrast, *Disabled-2*, whose gene product is thought to be involved in vesicle endocytosis, exhibits an antiphase pattern of transcription, with a nadir at CT14. A final group of genes, four members of the solute transporter family (*Slc12a2*, *Slc16a1*, *Slc19a1*, *Slc25a11*), show widely varying phases and amplitudes of cyclical gene expression (Figure 4E). This illustrates that functionally related genes are not necessarily expressed in the same circadian phase and raises the possibility that functional cascades are subject to temporally fine-grained circadian regulation.

Discussion

Genome-based analyses of circadian transcription conducted in plants and insects have largely focused on commercially available gene chips based on oligonucleotide sequences [16, 20, 21], although EST-based arrays have been applied to examine circadian expression patterns in *Arabidopsis* [17]. Our novel strategy utilized a cDNA-based array, customized for analysis of mouse liver function, to conduct two independent forms of simultaneous comparison (anchored and moving window) of RNA samples harvested across the circadian cycle. This dual approach to the identification of cycling transcripts affords enhanced rigour and objectivity. Its success was confirmed by its identification of the canonical clock genes *mPer1-3* and *Bmal1*. Our array-derived results were further validated by two independent rounds of in situ hybridization analyses of circadian gene expression for canonical clock genes and for three novel genes that showed very modest amplitudes. Our strategy provides a new and effective template for future transcriptome analyses using larger gene arrays, not least because it is able to identify, with statistical cross-validation, cycles of relatively low amplitude. To further underscore the effectiveness of our approach, we have compared our results with a recent microrray analysis of circadian transcription in mammalian fibroblasts (Duffield et al., this issue [44]). There was an impressive

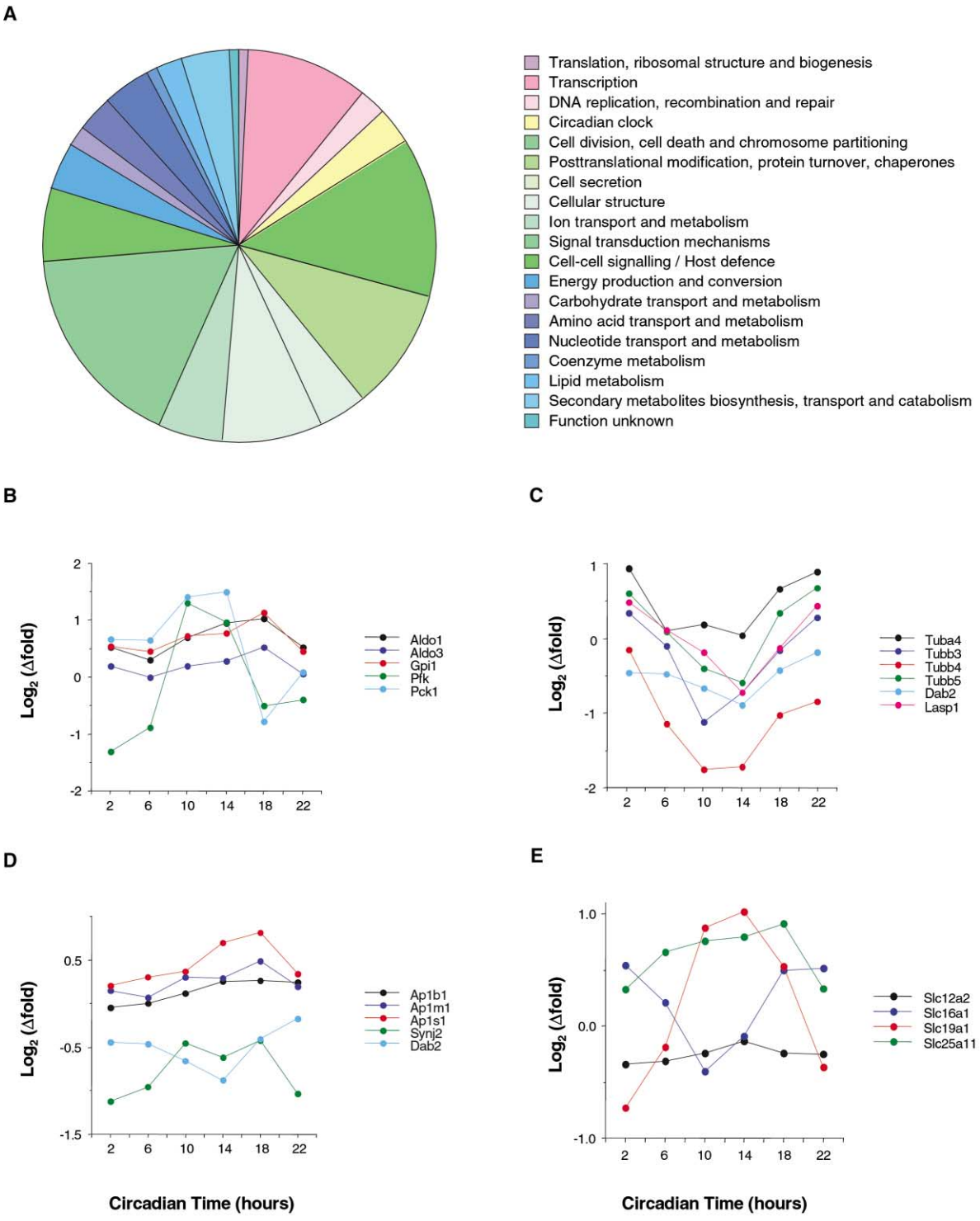

Figure 4. Functional Classification of Novel Circadian Transcripts

(A) Pie chart showing the distribution of all novel cycling genes (no ESTs) by molecular function. The key shows the molecular categories used to classify novel transcripts. The classification system used is based on the clusters of orthologous groups (COGs) system (see http://www.ncbi.nlm.nih.gov/COG). A combination of annotated function (Mouse Genome Database [MGD] and NCBI LocusLink) and literature searches was used to allocate genes to particular molecular classification group.

(B–E) Representative functional clusters of genes. (B) Genes involved in glycolysis and gluconeogenesis (*Aldo1*, *Aldo3*, *Gpi1*, *Pfk-2*, and *Pck1*). (C) Genes encoding cytoskeletal proteins (*Tuba4*, *Tubb3*, *Tubb4*, *Tubb5*, *Dab2*, and *Lasp1*). (D) Transcripts associated with vesicle trafficking and endocytosis (*Ap1b1*, *Ap1m1*, *Ap1s1*, *Synj2*, and *Dab2*). (E) Genes coding for some members of the solute carrier transporter family (*Slc12a2*, *Slc16a1*, *Slc19a1*, and *Slc25a11*).

correspondence between the two studies, in that of 13 novel cycling genes (or close family members) that were common to our study, ten were rhythmic in our analysis, and the other three were on our "reserve" list, just failing to reach our statistical criteria for inclusion (see Tables S1 and S3).

Our observation that ~9% of transcripts were circadian regulated is rather higher than the value of 2%–6% reported from studies examining different species and tissues and may reflect the customized gene set designed specifically for liver transcripts and our statistical inclusion of low-amplitude rhythms. If an amplitude threshold of 2-fold is applied, then the total would fall to ~4%, similar to that reported in *Arabidopsis* and *Drosophila* [16, 17, 20, 21]. However, our in situ hybridization analysis of three novel genes with amplitudes <2-fold, reveal the conservatism of this threshold and thus the underestimation of the true extent of the circadian transcriptome. Whether cycling mRNA leads to cycling protein levels, particularly for low-amplitude mRNA oscillations, remains to be seen. It is nevertheless interesting to note that changes in gene expression levels of considerably less than 1.5-fold, that are readily generated using different transformant lines of *Drosophila* carrying the *period* transgene (and whose transcript also cycles), produce quantifiable phenotypic changes [22].

Of the highest amplitude cycles observed, canonical clock genes were disproportionately represented, a finding consistent with global circadian transcription in *Drosophila* heads [20, 21]. The higher amplitude cycling genes tended to peak at subjective dawn and dusk, whereas the peaks of lower amplitude cycles had a very strong tendency to occur later at night. This suggests that within the liver's temporal wave of transcriptional activation, such low-amplitude genes might perhaps reside at the bottom of a circadian regulatory network, so that a temporal delay is inevitable because of their dependence on the cycling transcription (and translation) of upstream components. If so, it may be a general rule that the amplitude of the central molecular oscillator is dissipated down the individual clock-controlled networks rather than "geared up." Perhaps when a more comprehensive transcriptional analysis is performed (we have only assayed ~5% of the murine transcriptome) a clearer picture may emerge from the biochemical pathways in which many components cycle. One such pathway is the *Arabidopsis* phenylpropanoid cascade, in which the controlling transcription factor *PAP1* appears to show the third highest amplitude among 18 cycling genes, many of which appear to have very modest amplitudes [16]. Indeed, we provide evidence that similar circadian coordination also exists in the mammalian liver.

Circadian Control of Liver Glucose Metabolism

Numerous genes involved in liver metabolism, including enzymes and transporters (see Table S3 and Figure 4A), were rhythmic, consistent with reports of circadian rhythms in activity of some glycolytic enzymes and the citric acid cycle [23, 24]. In particular, we found robust, high-amplitude transcript cycling of the bifunctional enzyme *Pfk-2* (*phosphofructokinase-2/fructose-2,6-bisphosphatase*), a key control point in both glycolysis and gluconeogenesis. Circadian transcriptional regulation of metabolic enzymes and the mechanisms controlling their patterning await further clarification. The cycles may be an indirect consequence of circadian regulation of ingestion and/or a direct circadian control, mediated by neural and neuroendocrine links from the SCN. Under normal circumstances, direct circadian programming of the glycolysis and gluconeogenic pathway would complement homeostatic regulation driven by ingestion. For example, transcript levels for *Pfk-2* peaked at CT10, before the onset of the active period of the animal and presumably independently of feeding. Expression of *Pck1* (*phosphoenolpyruvate carboxykinase 1*), an enzyme intimately involved in gluconeogenesis, also peaks at the subjective day/night transition and may share a similar circadian regulation. The finding that other enzymes in the glycolysis pathway (e.g., *Aldo1/3* [*aldolase*] and *Gpi1* [*glucose phosphate isomerase1*]; see Figure 4B) peak together at CT20, toward the end of the active phase, suggests that circadian upregulation may reflect a combination of direct circadian programming and an indirect, homeostatic response to ingestion, as demonstrated for the expression of *Per1* in the liver, which is acutely sensitive to feeding schedule [25, 26].

Circadian Control of Cellular Vesicle Trafficking and Cytoskeletal Structure

Several genes encoding proteins involved in endocytosis also exhibited circadian rhythms in their expression (Figure 4D). Levels of *Synj2* (*synaptojanin* 2) are maximal between CT10-18, while another gene, *Dab2* (*Disabled-2*), peaks at CT22 (see Figure 4D). *Synaptojanin 2* is a recently characterized inositol 5-phosphatase involved in clathrin-mediated endocytosis of receptors [27]. *Disabled-2*, a protein believed to be involved in many aspects of vesicle trafficking and cytoskeletal integrity, has been linked to endocytosis of low-density lipoprotein receptors (LDLRs) [28]. The LDLR is essential for the uptake of lipids into hepatocytes, which occurs predominantly through clathrin-mediated endocytosis. It is therefore possible that uptake of lipoproteins from the blood is under circadian control. The finding that transcripts encoding three (out of four) components of the adaptor protein-1 (AP-1) complex (*Ap1b1*, *Ap1m1*, and *Ap1s1*) oscillate in phase suggests that there may also be circadian control over vesicle trafficking within the cell (see Figure 4D). The AP-1 complex is important in protein sorting and receptor recycling (e.g., LDLRs). Specifically, AP-1 is involved in trafficking between the trans-Golgi network (TGN) and the cell surface [29]. Thus, both receptor-mediated endocytosis and recycling of endocytosed receptors may be coordinated by the circadian clock.

Expression of many genes encoding key cytoskeletal elements is circadian in nature. Moreover, they oscillate in phase (see Figure 4C). Among them are four tubulin subunits (*Tuba4*, *Tubb3*, *Tubb4*, and *Tubb5*), heterodimeric polymers of which produce functional microtubules. If microtubule formation in cells throughout the liver is coordinated by the circadian system and accounting for the time lag between mRNA and protein

production, we can predict that α-tubulin and β-tubulin proteins achieve highest levels at CT6, the midpoint of the rest phase. Microtubules perform key functions in cell division, and a testable hypothesis is that extensive microtubule formation is related to the cycle of cell division, with mitotic spindle formation occurring principally at CT6. The recent finding that cell cycle regulators *cyclin D3* and *cdk4* undergo circadian oscillation in synchronized fibroblasts [30] and that we observed oscillation in cell cycle genes (e.g., *cyclin D1*) supports this hypothesis.

Circadian Control of Detoxification

Detoxification is an essential role of the liver, and, perhaps not surprisingly, we observed circadian oscillation of genes whose products are involved in this vital process. The cytochrome P450 genes are a highly conserved superfamily of monooxygenase enzymes involved in catalyzing a variety of cellular processes, including steroid synthesis and detoxification [31]. Among our set of cycling genes were three cytochrome P450 genes, including *Cyp17* and *Cyp2a4* (important in steroid synthesis) and *Cyp2e1*, a key detoxification enzyme localized to the endoplasmic reticulum [32]. Furthermore, *Gstt2* (*glutathione-S-transferase theta 2*), another pivotal detoxification enzyme [33], oscillates in phase with the cytochrome P450 genes. All showed subjective nighttime peaks between CT14-18. Close relatives of these genes have been found to be clock regulated in the head of *Drosophila*, probably emanating from the fat body [20, 21]. It is interesting to note that two of the above enzymes (*Cyp17* and *Gstt2*) have recently been linked to the pathogenesis of breast and prostate cancer [34, 35]. Circadian disruption of the SCN pacemaker, as occurs for example in shift work, may lead to a dampening of rhythms in these key effectors, putting individuals at greater risk from environmental carcinogens. Indeed, recent evidence suggests that chronic shift work and its attendent circadian disruption is associated with an increased risk of breast cancer [36].

Conservation of Circadian Genes across Species

From an evolutionary perspective, it is interesting to highlight similar genes and pathways between different species. Studies in *Drosophila* suggested a relationship between the clock and the immune system [20]. Such a possible link is also reflected in our data set with the *interleukin-1 receptor type 1* (*Il1r1*), which cycles with a 3-fold amplitude peaking at CT14. At this time (CT14-18), we also find peaks of two members of the Ras/MAPK family, *Map2k3* and *Mapk14*. Circadian control over elements of this cell signaling pathway have also been identified in *Drosophila* [20, 37]. Finally, proteasome subunit β10 (*Psmb10*), genes encoding *ubiquitin conjugating enzyme 7* (*Ubce7*) and its interacting partner 3 (*Ubce7ip3*), are coordinately regulated, peaking in the middle of the night (at CT18), with *ubiquitin specific protease 2* (*Usp2*) peaking about 8–10 hr earlier. Thus there appears to be a considerable time interval between the turnover of ubiquitin and subsequent ubiquitination. These results extend, in a more general way, the specific role of protein turnover in circadian timing in *Drosophila* [1].

Conclusions

The expression of rhythmicity at transcriptional and presumably also at posttrancriptional levels indicates that a host of hepatic functions are under tight circadian control, coordinated to the animal's behavior and the solar cycle. Rhythmic liver *mPer2* expression in rats is dependent on the SCN [38]. The current study reveals the SCN to be necessary for genome-wide circadian transcriptional control, confirming the pivotal role of this central pacemaker in driving peripheral rhythms. Our surgical approach has a key advantage over previous array studies conducted in clock mutant flies [20, 21] because the genetic components of the circadian clock machinery of the liver are not compromised by SCN ablation. Consequently, any loss of circadian patterning is due to the loss of the central pacemaker, without the confounding effects of genetic mutation within the liver. As noted earlier, the SCN can exert circadian control over the liver in several, interlinked ways. First, by maintaining a circadian rhythm of rest/activity and thereby of feeding, periodic satiety and fasting may be the primary driving factor [25, 26]. Second, the SCN drives circadian neuroendocrine rhythms such as the cycle of adrenocorticoid secretion [2], and this in turn may drive liver gene expression [39]. Finally, the SCN has extensive neural connections with the autonomic nervous system [40], which are well placed to regulate visceral function, including hepatic gene expression. It is very likely that all three influences (behavioral, endocrine, and autonomic) serve to consolidate SCN-dependent circadian regulation of the liver and other viscera. Both the intracellular signaling pathways and the *trans*-acting factors and *cis*-acting regulatory elements on which they operate to effect circadian patterns of gene activity may be important therapeutic targets for systemic diseases associated with circadian dysfunction arising from shift work, jet lag, and sleep disorders [3, 4, 5].

Experimental Procedures

Animal experimentation was licensed by the Home Office under the Animals (Scientific Procedures) Act, 198b. Adult male CD-1 mice (Harlan-Olac) were caged in groups of eight, in sound-proofed, ventilated environmental chambers under a lighting schedule of 12 hr bright white light and 12 hr dim red light (12L:12DR). To confirm entrainment and to monitor free-running activity rhythms on release into continuous dim red light (DR:DR), spontaneous locomotion was monitored by passive infrared movement detectors and recorded on a PC running Dataquest IV software (DataSciences, Frankfurt, Germany). Bilateral electrolytic lesion of the SCN was performed under general anesthesia (Rompun/Vetalar, Veterinary Drug Co.), using an insulated gauge 0 insect pin directed stereotaxically at the SCN. Coordinates used were on bregma, ± 0.20 mm from midline and 5.5 mm from the dural surface. Current applied was 1mV for 4 s. Actograms from intact and lesioned animals held in DR:DR were subjected to χ^2 periodogram analysis using the *Clocklab* analysis program (Actimetrix Inc., Evanston, Illinois) to confirm the absence of a free-running circadian competence. Liver and hypothalamus tissues were harvested from mice on the second cycle after transfer to DR:DR and immediately frozen prior to RNA extraction or sectioning for in situ hybridization (ISH). ISH was conducted and quantified as described previously [41], using specific antisense riboprobes to each gene (appropriate sense probes gave no

hybridization). Circadian patterning, the effect of SCN ablation, and any interactions between these factors were tested by one- and two-way analyses of variance (ANOVA), as appropriate.

Microarrays

cDNA microarrays based on the PCR products of IMAGE clones and generated by the Centre for Mechanisms of Human Toxicology at Leicester University (CMHT) were printed on poly-L-lysine-coated glass slides, using a Stanford-type arrayer [42]. Total RNA was extracted from liver, using RNeasy Maxi Kits (Qiagen). Equal amounts of liver tissue from four mice were pooled, and labeling, hybridization, and primary analysis were carried out according to reference [42]. Feature sizes, background, and feature fluorescence were calculated using GenePix 3.0 software (Axon Instruments). Median fluorescence for the pixels within the feature was calculated, and the raw data for each channel were then normalized by reference to the median fluorescence of the total feature set for that channel, and a $\log_2$(Cy5/Cy3) ratio was calculated. cDNAs on the glass slide were not randomly chosen but reflected the ongoing interests of CMHT, and many of the genes had duplicate copies on the slide, allowing further testing of the internal consistency of the hybridization. A number of clock genes and clock-controlled genes whose mRNAs cycle were present and served to validate our procedures. All genes that gave cycling patterns of expression were resequenced to confirm their identity.

Hybridization to the Microarray

We used two different experimental paradigms utilizing the ratio of hybridization of Cy5 and Cy3 fluorophores. In the anchored comparison, 50 μg of liver RNA from CT0 (Cy3, green) was compared with 50 μg of RNA harvested at 4 hr intervals between CT2 and 26 (Cy5, red) ($n = 4$ mice each). Our second, independent strategy used a moving 12 hr window design in which mRNA pools from two different times, 12 hr apart, collected under the same DR conditions, were compared (CT 2/14, 4/16, 6/18, 8/20, 10/22, 12/24, 14/26), again, using four livers per time point. This would be more useful for detecting low-amplitude oscillations, as a peak and trough could be hit simultaneously, thereby providing a larger Cy5/Cy3 ratio than the anchored method, which is dependent solely on CT0 mRNA levels for the overall pattern. In a final experiment, 12 SCN-lesioned mice were sacrificed at CT0 and six each at CT6, CT12, and CT18, RNA prepared from their livers, labeled with the fluorophores, and CT0/CT6 and CT0/CT18 samples were hybridized to the arrays. CT6/18 and CT0/12 moving window comparisons, harvested in the same way from SCN ablated animals, were also compared. Hybridizations to the slides were performed simultaneously for the different time points within each experiment [42]

Statistical Analysis

To be considered "cycling," a gene had to give a pattern consistent with rhythmicity by both anchored and moving window methods. The Cy5/Cy3 anchored data, in $\log_2$ units, was analyzed using the CLEAN spectral method, and associated Monte Carlo simulations provided stringent 95% confidence limits for such a limited number of data points [43]. Periods within 17–35 hr were accepted as being within the circadian range. The first six time points of the moving window data, for a sinusoid peaking at CT2/26, will generate a straight line moving from negative (green Cy3) to positive (red Cy5) values and give a statistically significant positive correlation, $+$R1. Similarly, a sinusoid peaking at CT14 will generate a significant negative correlation, $-$R1. Significant cross-correlations to an underlying sinusoid can thus be obtained by phase shifting the data for each gene through every time point and generating six correlations, R1–R6. Any sinusoid can be identified, simply by inspecting the characteristic pattern of the R1–R6 correlogram, which provides an independent determination of rhythmicity and phase. A gene whose anchored data revealed a significant spectral analysis (beyond 95% confidence limit) and a period within the circadian range was inspected for its phase, and then the correlogram was scrutinized for any corresponding significant R1–R6 values (one-tailed). Conversely, any gene that showed a significant correlogram (two-tailed) was then inspected for its spectrogram, using the corresponding one-tailed 95% significance value from the Monte Carlo analysis. Genes that showed significant spectral analyses and corresponding correlograms were classified as rhythmic. Patterns of gene expression were visualized using CLUSTER and TREEVIEW software (http://rana.lbl.gov/EisenSoftware.htm) [18].

Supplementary Material

Supplementary Table S1 shows the list of cycling liver genes, accession numbers, spectral periods, and fold amplitude, plus the cross-correlations R1-R6 for each gene, and the comparison with the results of Duffield et al. [44]. Table S2 gives the raw log2 Cy5/Cy3 ratios for the different time points for both anchored and moving window comparisons for each locus. Finally, Table S3 provides the same genes divided into functional groups with accession numbers and the circadian expression cluster into which they fell (see Figure 1). The Supplementary Material can be found online at http://images.cellpress.com/supmat/supmatin.htm.

Acknowledgments

The authors are grateful to J. Bashford, I. Bolton, and A. Newman for their expert assistance in photomicrography and image analysis. We also thank R. Davies for assistance with clone sequencing; and Michael Lush for help with bioinformatics. Finally, we thank G. Duffield and J. Dunlap for sharing unpublished data. This work was supported by the Biotechnology and Biological Sciences Research Council (Project Grant to M.H.H. and C.P.K.) and the Human Frontiers Science Programme (grant to C.P.K.).

Received: December 24, 2001
Revised: February 8, 2002
Accepted: February 8, 2002
Published: April 2, 2002

References

1. Dunlap, J.C. (1999). Molecular bases for circadian clocks. Cell *96*, 271–290.
2. Weaver, D.R. (1998). The suprachiasmatic nucleus: a 25-year retrospective. J. Biol. Rhythms *13*, 100–112.
3. Costa, G. (1996). The impact of shift and night work on health. Appl. Ergonomics *27*, 9–16.
4. Hastings, M.H. (1998). The brain, circadian rhythms and clock genes. BMJ *317*, 1704–1707.
5. Rajaratnam, S.M.W., and Arendt, J. (2001). Health in a 24-h society. Lancet *358*, 999–1005.
6. Ivanchenko, M., Stanewsky, R., and Giebultowicz, J.M. (2001). Circadian photoreception in Drosophila: functions of cryptochrome in peripheral and central clocks. J. Biol. Rhythms *16*, 205–215.
7. Whitmore, D., Foulkes, N.S., and Sassone-Corsi, P. (2000). Light acts directly on organs and cells in culture to set the vertebrate circadian clock. Nature *404*, 87–91.
8. Balsalobre, A., Damiola, F., and Schibler, U. (1998). A serum shock induces circadian gene expression in mammalian tissue culture cells. Cell *93*, 929–937.
9. Yamazaki, S., Numano, R., Abe, M., Hida, A., Takahashi, R., Ueda, M., Block, G.D., Sakaki, Y., Menaker, M., and Tei, H. (2000). Resetting central and peripheral circadian oscillators in transgenic rats. Science *288*, 682–685.
10. Bell-Pedersen, D., Lewis, Z.A., Loros, J.J., and Dunlap, J.C. (2001). The Neurospora circadian clock regulates a transcription factor that controls rhythmic expression of the output eas(ccg-2) gene. Mol. Microbiol. *4*, 897–909.
11. Ripperger, J.A., Shearman, L.P., Reppert, S.M., and Schibler, U. (2000). CLOCK, an essential pacemaker component, controls expression of the circadian transcription factor DBP. Genes Dev. *14*, 679–689.
12. Zhu, H., Nowrousian, M., Kupfer, D., Colot, H.V., Berrocal-Tito, G., Lai, H., Bell-Pedersen, D., Roe, B.A., Loros, J.J., and Dunlap, J.C. (2001). Analysis of expressed sequence tags from two starvation, time-of-day-specific libraries of *Neurospora crassa* reveals novel clock-controlled genes. Genetics *3*, 1057–1065.
13. Van Gelder, R.N., Bae, H., Palazzolo, M.J., and Krasnow, M.A.

(1995). Extent and character of circadian gene expression in Drosophila melanogaster: identification of twenty oscillating mRNAs in the fly head. Curr. Biol. *5*, 1424–1436.
14. Kornmann, B., Preitner, N., Rifat, D., Fleury-Olela, F., and Schibler, U. (2001). Analysis of circadian liver gene expression by ADDER, a highly sensitive method for the display of differentially expressed mRNAs. Nucleic Acids Res. *29*, E51.
15. Liu, Y., Tsinoremas, N.F., Johnson, C.H., Lebedeva, N.V., Golden, S.S., Ishiura, M., and Kondo, T. (1995). Circadian orchestration of gene expression in cyanobacteria. Genes Dev. *9*, 1469–1478.
16. Harmer, S.L., Hogenesch, J.B., Straume, M., Chang, H.S., Han, B., Zhu, T., Wang, X., Kreps, J.A., and Kay, S.A. (2000). Orchestrated transcription of key pathways in Arabidopsis by the circadian clock. Science *290*, 2110–2113.
17. Schaffer, R., Landgraf, J., Accerbi, M., Simon, V.V., Larson, M., and Wisman, E. (2001). Microarray analysis of diurnal and circadian-regulated genes in *Arabidopsis*. Plant Cell *1*, 113–123.
18. Eisen, M.B., Spellman, P.T., Brown, P.O., and Botstein, D. (1998). Cluster analysis and display of genome-wide expression patterns. Proc. Natl. Acad. Sci. USA *95*, 14863–14868.
19. Oishi, K., Sakamoto, K., Okada, T., Nagase, T., and Ishida, N. (1998). Antiphase circadian expression between BMAL1 and period homologue mRNA in the suprachiasmatic nucleus and peripheral tissues of rats. Biochem. Biophys. Res. Commun. *253*, 199–203.
20. MacDonald, M.J., and Rosbash, M. (2001). Microarray analysis and organisation of circadian gene expression in *Drosophila*. Cell *107*, 567–578.
21. Claridge-Chang, A., Wijnen, H., Naef, F., Boothroyd, C., Rajewsky, N., and Young, M.W. (2001). Circadian regulation of gene expression systems in the *Drosophila* head. Neuron *32*, 657–671.
22. Baylies, M.K., Bargiello, T.A., Jackson, F.R., and Young, M.W. (1987). Changes in abundance or structure of the *per* gene product can alter periodicity of the *Drosophila* clock. Nature *326*, 390–392.
23. Feuers, R.J., Casciano, D.A., Tsai, T.H., and Scheving, L.E. (1987). Regulation of the circadian rhythm of hepatic pyruvate kinase in mice. Prog. Clin. Biol. Res. *227A*, 163–172.
24. Kaminsky, Y.G., and Kosenko, E.A. (1987). Diurnal rhythms in liver carbohydrate metabolism. Comparative aspects and critical review. Comp. Biochem. Physiol. B *86*, 763–784.
25. Damiola, F., le Minh, N., Peritner, N., Kornmann, B., Fleury-Olela, F., and Schibler, U. (2000). Restricted feeding uncouples circadian oscillators in peripheral tissues from the central pacemaker in the suprachiasmatic nucleus. Genes Dev. *14*, 2950–2961.
26. Stokkan, K.A., Yamazaki, S., Tei, H., Sakaki, Y., and Menaker, M. (2001). Entrainment of the circadian clock in the liver by feeding. Science *291*, 490–493.
27. Malecz, N., McCabe, P.C., Spaargaren, C., Qiu, R., Chuang, Y., and Symons, M. (2000). Synaptojanin *2*, a novel Rac1 effector that regulates clathrin-mediated endocytosis. Curr. Biol. *10*, 1383–1386.
28. Morris, S.M., and Cooper, J.A. (2001). Disabled-2 colocalizes with the LDLR in clathrin-coated pits and interacts with AP-2. Traffic *2*, 111–123.
29. Marsh, M., and McMahon, H.T. (1999). The structural era of endocytosis. Science *285*, 215–220.
30. Grundschober, C., Delaunay, F., Puhlhofer, A., Triqueneaux, G., Laudet, V., Bartfai, T., and Nef, P. (2001). Circadian regulation of diverse gene products revealed by mRNA expression profiling of synchronized fibroblasts. J. Biol. Chem. *276*, 46751–46758.
31. Lin, J.H., and Lu, A.Y. (2001). Interindividual variability in inhibition and induction of cytochrome P450 enzymes. Annu. Rev. Pharmacol. Toxicol. *41*, 535–567.
32. Cederbaum, A.I., Wu, D., Mari, M., and Bai, J. (2001). CYP2E1-dependent toxicity and oxidative stress in HepG2 cells(1,2). Free Radic. Biol. Med. *31*, 1539–1543.
33. Landi, S. (2000). Mammalian class theta GST and differential susceptibility to carcinogens: a review. Mutat. Res. *463*, 247–283.
34. Spurdle, A.B., Hopper, J.L., Dite, G.S., Chen, X., Cui, J., McCredie, M.R., Giles, G.G., Southey, M.C., Venter, D.J., Easton, D.F., et al. (2000). CYP17 promoter polymorphism and breast cancer in Australian women under age forty years. J. Natl. Cancer Inst. *92*, 1674–1681.
35. Change, B., Zheng, S.L., Isaacs, S.D., Wiley, K.E., Carpten, J.D., Hawkins, G.A., Bleecker, E.R., Walsh, P.C., Trent, J.M., Meyers, D.A., et al. (2001). Linkage and association of CYP17 gene in hereditary and sporadic prostate cancer. Int. J. Cancer *95*, 354–359.
36. Schernhammer, E.S., Laden, F., Speizer, F.E., Willett, W.C., Hunter, D.J., Kawachi, I., and Colditz, G.A. (2001). Rotating night shifts and risk of breast cancer in women participating in the nurses' health study. J. Natl. Cancer Inst. *93*, 1563–1568.
37. Williams, J.A., Su, H.S., Bernards, A., Fields, J., and Sehgal, A. (2001). A circadian output in *Drosophila* mediated by Neurofibromatosis-1 and Ras/MAPK. Science *293*, 2252–2256.
38. Sakamoto, K., Nagase, T., Fukui, H., Horikawa, K., Okada, T., Tanaka, H., Sato, K., Miyake, Y., Ohara, O., Kako, K., et al. (1998). Multitissue circadian expression of rat period homolog (rPer2) mRNA is governed by the mammalian circadian clock, the suprachiasmatic nucleus in the brain. J. Biol. Chem. *273*, 27039–27042.
39. Balsalobre, A., Brown, S.A., Marcacci, L., Tronche, F., Kellendonk, C., Reichardt, H.M., Schutz, G., and Schibler, U. (2000). Resetting of circadian time in peripheral tissues by glucocorticoid signalling. Science *289*, 2344- 2347.
40. Buijs, R.M., and Kalsbeek, A. (2001). Hypothalamic integration of central and peripheral clocks. Nat. Rev. Neurosci. *2*, 521–526.
41. Maywood, E.S., Mrosovsky, N., Field, M.D., and Hastings, M.H. (1999). Rapid down-regulation of mammalian period genes during behavioral resetting of the circadian clock. Proc. Natl. Acad. Sci. USA *96*, 15211–15216.
42. Turton, N.J., Judah, D.J., Riley, J., Davies, R., Lipson, D., Styles, J.A., Smith, A.G., and Gant, T.W. (2001). Gene expression and amplification in breast carcinoma cells with intrinsic and acquired doxorubicin resistance. Oncogene *20*, 1300–1306.
43. Kyriacou, C.P., and Hall, J.C. (1989). Spectral analysis of *Drosophila* courtship song rhythms. Anim. Behav. *37*, 850–859.
44. Duffield, G.E., Best, J.D., Meurers, B.H., Bittner, A., Loros, J.J., and Dunlap, J.C. (2002). Circadian programs of transcriptional activation, signaling, and protein turnover revealed by microarray analysis of mammalian cells. Curr. Biol. *12*, 551–557.